Preparation and Surface Science Characterization of Model Ziegler−Natta Catalysts. Role of Undercoordinated Surface Magnesium Atoms in the Chemisorption of $TiCl_4$ on $MgCl_2$ Thin Films

Enrico Magni and Gabor A. Somorjai*

Department of Chemistry, University of California, Berkeley, California 94720-1460, and Materials Sciences Division, Lawrence Berkeley National Laboratory, University of California, Berkeley, California 94720

Received: April 27, 1998; In Final Form: July 31, 1998

Two new synthetic routes for the preparation of model Ziegler−Natta catalysts under UHV conditions are described. The exposure of metallic magnesium to $TiCl_4$ produced titanium chloride films with Ti in the 4+, 3+, 2+, and 0 oxidation states. Stable titanium chloride films could also be obtained by $TiCl_4$ and Mg codeposition on $MgCl_2$ and Au. A $TiCl_4/TiCl_2$ film was obtained in this case. The reaction of these systems with $AlEt_3$ produced model catalysts for the polymerization of both ethylene and propylene. XPS is a proper technique for the characterization of the oxidation state of Ti in a variety of titanium chloride surface species. The stability of $MgCl_2$ surfaces with a high concentration of undercoordinated Mg atoms was studied in UHV by Mg gas-phase deposition on a $MgCl_2$ multilayer film. The Mg adatoms were readily coordinated by the Cl ions diffusing from the halide bulk to the surface. Mg-containing $MgCl_2$ faces are thermodynamically unstable, and the fast diffusion of the Cl ions in the $MgCl_2$ matrix allows the recovery of the chlorine termination to lower the system surface energy. The high mobility of the chlorine ions is of central importance for the molecular level understanding of the dynamic equilibrium among the $MgCl_2$ surface, $TiCl_4$, and the electron donors used in the synthesis of high performance microporous Ziegler−Natta catalysts. The deposition of $MgCl_2$ in the presence of $TiCl_4$ was studied for the stabilization of high Miller index faces during the $MgCl_2$ film growth. The interaction between the two halides is too weak to influence the $MgCl_2$ deposition, and $TiCl_4$ could not be chemisorbed at 300 K.

1. Introduction

Ziegler−Natta catalysts are used for the polymerization of α-olefins such as ethylene and propylene. The precursor of the active site is obtained by the chemisorption of $TiCl_4$ on highly disordered $MgCl_2$. The titanium chloride is then reduced and alkylated by the reaction with an aluminum alkyl to produce the active center. It has been suggested that, during the preparation of the microporous catalyst using conventional synthetic techniques, the $TiCl_4$ is chemisorbed on the undercoordinated Mg atoms exposed at the lateral cuts of the $MgCl_2$ crystallites. In particular, the tetra- and pentacoordinated Mg atoms present at the (110) and (100) faces of $MgCl_2$ are thought to be the binding sites for $TiCl_4$.[1−4]

In this paper, we report the results of our detailed study of the interaction between the $TiCl_4$ molecules and the surface of $MgCl_2$ films prepared under controlled conditions. We specifically focused our attention on the role of the surface Mg atoms. Model Ziegler−Natta catalysts were prepared under ultra-high-vacuum (UHV) conditions by gas-phase deposition of $MgCl_2$ and $TiCl_4$ on a gold foil. The surface concentration of Mg atoms was controlled by gas-phase deposition. The titanium chloride films thus obtained were reduced and alkylated by reaction with $AlEt_3$ to form the active sites. The model surfaces were characterized by X-ray photoelectron spectroscopy (XPS), ion scattering spectroscopy (ISS), and polymerization activity tests.

We studied the deposition of $TiCl_4$ on metallic magnesium and monitored by XPS the reduction of the halide at the metal surface. This reaction produced a titanium chloride film in which the Ti was in the 0, 2+, 3+, and 4+ oxidation states. The exposure of this system to $AlEt_3$ produced an active catalyst for the polymerization of both ethylene and propylene. Active model Ziegler−Natta catalysts were also obtained by Mg and $TiCl_4$ codeposition on either $MgCl_2$ or Au, followed by reduction and alkylation with $AlEt_3$. During the codeposition experiment, a redox reaction between the deposited Mg atoms and the $TiCl_4$ molecules impinging from the gas phase allowed for the deposition of a titanium chloride film. This film was very similar in composition to the one obtained by electron irradiation induced chemical vapor deposition of $TiCl_4$ on the same substrates.[5−8]

The $MgCl_2$ films grown under UHV conditions expose only Cl atoms at the solid−vacuum interface. Gas-phase $TiCl_4$ molecules do not chemically interact with these films.[9−12] The stability of $MgCl_2$ surfaces containing undercoordinated Mg sites was studied at room temperature by the gas-phase deposition of Mg atoms on the halide surface. ISS and XPS analyses indicated that the deposited Mg atoms were rapidly coordinated by the Cl atoms diffusing to the surface from the subsurface layers of the $MgCl_2$ film. The concentration of Mg atoms at the solid−vacuum interface was below the detection limit after the deposition of 10^{16} Mg atoms/cm^2.

Finally, we studied the possibility of increasing the sticking probability of $TiCl_4$ to $MgCl_2$ by simultaneous exposure of the magnesium chloride films to $TiCl_4$ and $MgCl_2$ molecular beams. In this experiment, our goal was the preferential growth of faces of $MgCl_2$ other than the basal plane. Very little $TiCl_4$ was deposited under these conditions.

* To whom correspondence should be addressed at the Department of Chemistry. Fax: +1 510 643 9668. E-mail: somorjai@socrates.berkeley.edu.

10.1021/jp982017y CCC: $15.00
Published on Web 10/13/1998

2. Experimental Section

The UHV apparatus and experimental procedure used in the present study have been described in detail elsewhere.[5,6] Briefly, the apparatus consisted of a preparation chamber, maintained at a background pressure of 1×10^{-9} Torr by an ion pump, coupled with a PHI 5400 Small Spot ESCA analysis system and a reaction cell, where gases and liquids were introduced near atmospheric pressure. The sample under study was transferred from one section of the apparatus to the others without exposure to air or any other contaminant through a series of gate valves and transfer arms. The preparation chamber was equipped with a Knudsen cell that produced a beam of $MgCl_2$ molecules used for the growth of clean films of controlled thickness. A second Knudsen cell allowed for the sublimation of metallic magnesium and the production of a Mg atomic beam. The temperature of both sources was adjusted in order to obtain the desired flux. A leak valve connected to a directed doser allowed for the introduction of a controlled pressure of $TiCl_4$ during the deposition of the titanium chloride film. The analysis chamber was provided with a non-monochromatic X-ray source, a hemispherical electron energy analyzer having a mean radius of 28 cm, and a differentially pumped ion gun. The electron analyzer was operated at fixed energy resolution using a pass energy of 8.9 or 71.5 eV as specified for each experiment reported. The reaction cell was directly connected to the source of $AlEt_3$ which was introduced either in the gas or in the liquid phase. After the reaction with $AlEt_3$, the cell was evacuated by a liquid-nitrogen sorption pump and a turbo molecular pump before transferring the sample to the UHV sections of the apparatus.

The elemental composition and the oxidation state of the atoms in the deposited films were monitored by XPS, using Al Kα excitation radiation (1486.6 eV) and detecting photoelectrons at a takeoff angle of 54°. The Au $4f_{7/2}$ peak at 84.0 eV was taken as a reference for the energy scale. The XPS peak areas are reported after correction by the corresponding sensitivity factors (Au $4f_{7/2}$, 3.5; Ti 2p, 2.0; Mg KLL, 2.4; Cl 2p, 0.89; C 1s, 0.30; O 1s, 0.71; Al 2s, 0.29)[13] and normalization with respect to the Au $4f_{7/2}$ peak area of the clean substrate set equal to 100. The atomic compositions were calculated from the integrated peak areas of XPS spectra collected at an electron pass energy of 71.5 eV, corrected by the corresponding sensitivity factors. We used the approximation that the surface composition was homogeneous over the analysis volume. From repeated experiments, we estimated the following relative random errors in the calculation of the atomic concentrations: Ti, 5%; Mg, 1%; Cl, 2%; Al, C, and O, 20%.

For each of the XPS spectra in the Ti 2p region, an attempt has been made to fit the experimental curve with a series of synthetic peaks that represent the contribution of the photoelectron emission from atoms in different chemical environments. Care has been taken to fit the experimental curves to the minimum number of peaks. These peaks are described as a mixture of Gaussian and Lorentzian contributions in order to take into consideration the effect of the instrumental error on the peak shape characteristic of the photoemission process. A certain degree of asymmetry is introduced to the peak shape to account for the tail present at the high binding energy side of the peak due to inelastic scattering of the photoelectrons during their transport to the sample surface and to the possible presence of shake-up features. The use of asymmetric curves allows us to assume a linearly sloping background. The tail is described by a non-negative term added to the high binding energy side of the mixed Gaussian and Lorentzian peak. This term is the convolution of an exponential function and a Gaussian peak.[14] The shape of each synthetic peak is fully identified by the percent Gaussian contribution (*G*), the full width at half-maximum (fwhm), the tail length (TL), and the tail scale (TS). The values of the shape parameters that characterize the eight peaks used for the curve fitting of our Ti 2p experimental signals are reported in Table 1. In all cases, $p_{1/2}$ peaks have areas exactly half of those of the respective $p_{3/2}$ peaks.

TABLE 1: Parameter Values for the Synthetic Curves Used in the Description of the Experimental Ti 2p XPS Peaks[a]

pass energy (eV)		$TiCl_4$		$TiCl_3$		$TiCl_2$		Ti	
		$p_{3/2}$	$p_{1/2}$	$p_{3/2}$	$p_{1/2}$	$p_{3/2}$	$p_{1/2}$	$p_{3/2}$	$p_{1/2}$
8.9	TL	14	18	14	18	13.5	18	14	18
	TS	0.6	0.6	0.6	0.6	0.55	0.5	0.5	0.5
	G	75	75	75	75	75	75	75	75
	fwhm	1.7	1.7	1.7	1.7	1.7	1.7	1.7	1.7
71.5	*G*	85	85			85	85		
	fwhm	1.9	1.9			1.9	1.9		

[a] *G* = percent of Gaussian Contribution; fwhm = full width at half-maximum; TL = tail length; TS = tail scale.

The chemical composition of the uppermost monolayer of the deposited films was analyzed by ISS, using He ions of 700 eV incident energy with a flux of 5×10^{12} ions/(cm^2 s). To minimize the damage to the surface under study, the incident ion beam was rastered on the sample surface and the data acquisition time limited to 3 min. These conditions allowed us to obtain spectra with good signal-to-noise ratios and negligible damage of the sample surface.

3. Results

3.1. Preparation of Model Ziegler−Natta Catalysts: $TiCl_4$ Deposition on Metallic Mg. A detailed analysis of the surface reaction between $TiCl_4$ and Mg is not reported in the literature. We studied the reduction of $TiCl_4$ on the Mg surface by gas phase deposition of the halide on metallic magnesium. Oxygen-free Mg surfaces can readily be obtained by sublimation of the metal and deposition from the gas phase on a gold foil. We prepared clean Mg films using a Knudsen cell with the Mg source at 650 K and maintaining the Au substrate at 300 K. A thick magnesium overlayer was deposited under these conditions after 60 min. The lower curves in Figure 1, parts a and b, respectively show the Mg KLL and the Mg 2p regions of the XPS spectrum of the Mg film. They are characteristic of metallic Mg, with the most pronounced of the Mg KLL peaks at 1185.5 eV and the Mg 2p peak at 50.0 eV, in agreement with the literature values.[7,10,13−19]

The exposure of this Mg film to $TiCl_4$ at a pressure between 1×10^{-7} and 1×10^{-6} Torr induced a fast redox reaction at the film surface. The Ti^{4+} was reduced to the 3+, 2+, and 0 oxidation states and the Mg was oxidized to $MgCl_2$. Parts a−c, respectively, of Figure 1 show the Mg KLL, Mg 2p, and Ti 2p regions of the XPS spectra recorded after the exposure of 10, 100, and 1000 L of $TiCl_4$. (The langmuir (L) is a practical unit of exposure defined as 1×10^{-6} Torr·s.) Table 2 summarizes the atomic compositions at the film surface after the different exposures. A small amount of O was accumulated at the film surface due to the high reactivity of Mg with oxygen-containing molecules present in the vacuum system during the $TiCl_4$ exposure. The surface reaction between Mg and $TiCl_4$ generated a new peak in the Mg KLL and in the Mg 2p regions of the XPS spectra, with maxima at 1178.9 and 53.0 eV. These peaks became stronger for larger $TiCl_4$ exposures and are due to the formation of $MgCl_2$.[7,10,20,21]

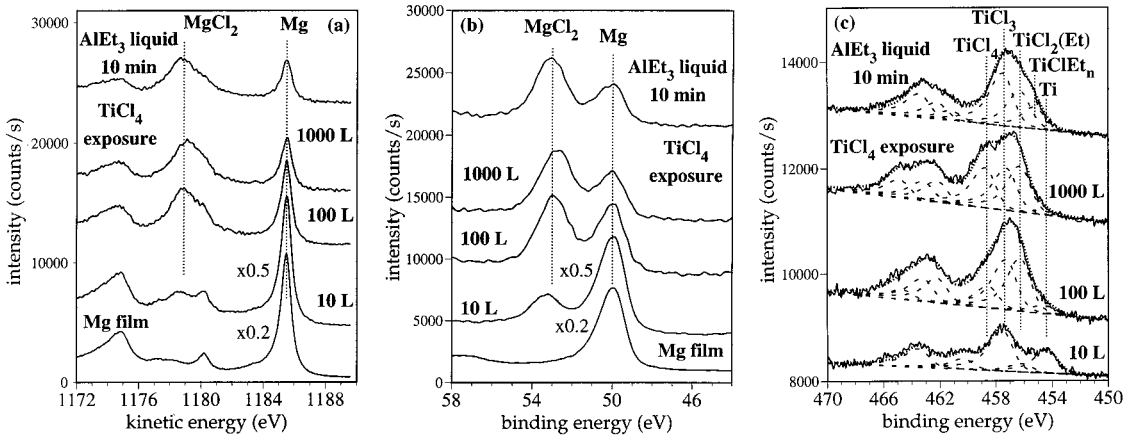

Figure 1. Mg film deposition on polycrystalline Au followed by the exposure to $TiCl_4$ and the reaction with $AlEt_3$. Mg KLL, Mg 2p, and Ti 2p regions of the XPS spectra are shown. Mg source temperature: 650 K. $TiCl_4$ pressure: from 1×10^{-7} to 1×10^{-6} Torr. $AlEt_3$ exposure: liquid layer for 10 min. Substrate temperature: 300 K. (a) Mg KLL peak. Detector pass energy: 8.9 eV. (b) Mg 2p peak. Detector pass energy: 71.5 eV. (c) Ti 2p region of the spectra and curve fitting. Detector pass energy: 8.9 eV.

TABLE 2: XPS Surface Atomic Compositions of the Mg Film after Exposure to $TiCl_4$ and $AlEt_3$

	atomic composition (%)					
model system	Ti	Mg	Cl	C	O	Al
Mg film		100				
$TiCl_4$ exposure						
10 L	10	46	41		3	
100 L	16	25	59			
1000 L	16	20	62		2	
$AlEt_3$ exposure						
liquid film/10 min	11	16	40	23	5	5

The oxidation of the Mg atoms was coupled with the reduction of the titanium in the $TiCl_4$ molecules sticking to the film surface. After the exposure of 10 L of $TiCl_4$, the surface atomic concentration of Ti was already 10%. The Ti 2p region of the XPS spectrum is dominated by a peak at 457.4 eV which, together with the peak at 463.3 eV, forms the spin−orbit doublet characteristic of Ti atoms in $TiCl_3$.[22] A second intense doublet is present at 454.4 and 460.5 eV, due to the $2p_{3/2}$ and $2p_{1/2}$ photoelectrons from zerovalent Ti atoms, eventually alloyed with the Mg film.[6] A third weak spin−orbit doublet is present, with maxima at 456.2 and 462.2 eV, due to the presence of a small amount of $TiCl_2$.[5−7] The Cl to Ti atomic ratio (Table 2) was 4:1, indicating that every Cl atom liberated from the $TiCl_4$ reduction stayed on the Mg surface forming Mg−Cl bonds. At larger $TiCl_4$ exposures, the $TiCl_2$ $2p_{3/2}$ and $2p_{1/2}$ peaks became stronger and two new peaks appeared at 458.6 and 464.7 eV. This is the spin−orbit doublet characteristic of $TiCl_4$.[5−7,22,23] At the same time, the Ti zerovalent peaks gradually disappeared. After the exposure of 1000 L of $TiCl_4$, the Ti atoms accounted for 16% of the film surface atomic composition; Ti^{4+}, Ti^{3+}, and Ti^{2+} were present in roughly the same amount. Incidentally, we underline the possibility to distinguish by XPS among Ti atoms simultaneously present at the sample surface in the 4+, 3+, 2+, and 0 oxidation states. This is of central importance for the characterization of the oxidation state of the titanium present in the stereoselective active site for the Ziegler−Natta polymerization.

The exposure of this titanium chloride film to a liquid layer of $AlEt_3$ at 300 K for 10 min produced the extensive reduction of the $TiCl_4$ to $TiCl_3$ and its partial alkylation products. This is suggested by the shape of the Ti 2p region of the XPS spectrum (Figure 1c). Our curve fitting indicates that the 458.6 and 464.7 eV components disappeared and the lower oxidation state peaks grew more intense. The upper limit of the amount of unreduced $TiCl_4$ after the $AlEt_3$ exposure can be estimated by eliminating the asymmetric component in the synthetic peak corresponding to $TiCl_3$ and introducing the $2p_{3/2}$ and $2p_{1/2}$ components of $TiCl_4$ in the fitting. In so doing, we calculated that $TiCl_4$ accounts for less than 11% of the total Ti present after the reduction−alkylation reaction. The C uptake is consistent with the formation of products of partial alkylation of the titanium chloride. $TiCl_2Et$ was probably present, but the corresponding Ti $2p_{3/2}$ peak at 456.2 eV overlaps with the peak due to $TiCl_2$. The appearance of the spin−orbit doublet at 455.2 and 461.2 eV is indicative of the formation of $TiClEt_n$, where n can be 1 and/or 2. All these features are consistent with our previous work in which we extensively monitored by XPS the surface reaction of a $TiCl_4/TiCl_2$ thin film with gas- and liquid-phase $AlEt_3$ at 300 K.[7]

The $TiCl_4/TiCl_3/TiCl_2$ film prepared by exposure of the Mg surface to $TiCl_4$ became an active catalyst for the Ziegler−Natta polymerization of α-olefins after the reduction−alkylation reaction with the aluminum alkyl. We tested the activity of this model catalyst by running gas-phase polymerization reactions in the presence of 760 Torr of monomer at 300 K. Both ethylene and propylene were polymerized.

3.2. Preparation of Model Ziegler−Natta Catalysts: $TiCl_4$ and Mg Codeposition on $MgCl_2$ and Au. Titanium chloride films were prepared by $TiCl_4$ and Mg codeposition on $MgCl_2$. In this experiment, we deposited 10 layers of $MgCl_2$ on the Au substrate and we exposed the film, held at 300 K, to simultaneous beams of $TiCl_4$ and Mg. The halide was introduced in the chamber at 2×10^{-7} Torr; this corresponds to a flux of 3×10^{13} $TiCl_4$ molecules/(cm^2 s). The flux of the magnesium beam was measured, as described in section 3.3, to be 3×10^{12} Mg atoms/(cm^2 s) at the target sample. Under these experimental conditions, about 10 $TiCl_4$ molecules hit the $MgCl_2$ surface per every Mg atom that adsorbed on it (assuming unitary sticking probability for Mg on $MgCl_2$ at room temperature). This large excess of $TiCl_4$ enhanced the probability for each Mg adatom to react with the titanium chloride. At the same time, the gas-phase collision probability between one Mg atom and one $TiCl_4$ molecule was of the order of 10^{-4}, which suggests a maximum deposition rate for products of gas-phase reaction of the order of 10^8 molecules/(cm^2 s).

Figure 2 shows the Mg KLL, Cl 2p, and Ti 2p regions of the XPS spectra acquired at different stages of the $TiCl_4$ and Mg codeposition. The Mg KLL and the Cl 2p peaks, initially at 1178.1 and 201.1 eV, gradually shifted to 1179.2 and 200.1 eV

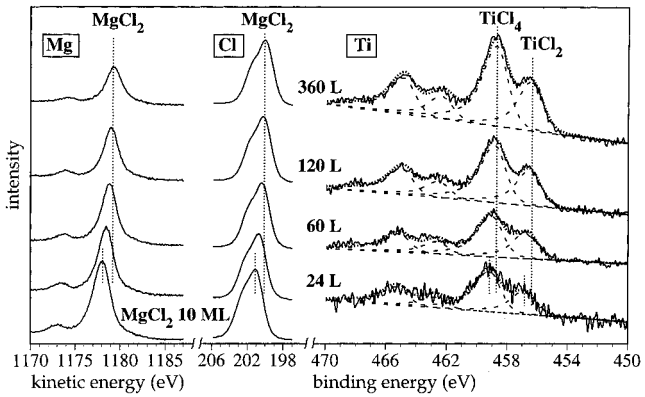

Figure 2. $TiCl_4$ and Mg codeposition on 10 layers of $MgCl_2$ film. Mg KLL, Cl 2p, and Ti 2p regions of the XPS spectra at different $TiCl_4$ exposures are shown. $TiCl_4$ pressure: 2×10^{-7} Torr. Mg flux: 3×10^{12} atoms/(cm^2 s). $TiCl_4$ to Mg molecular flux ratio at the target surface: 10:1. Substrate temperature: 300 K. Detector pass energy: 8.9 eV for the Mg KLL and the Ti 2p peaks; 71.5 eV for the Cl 2p peak.

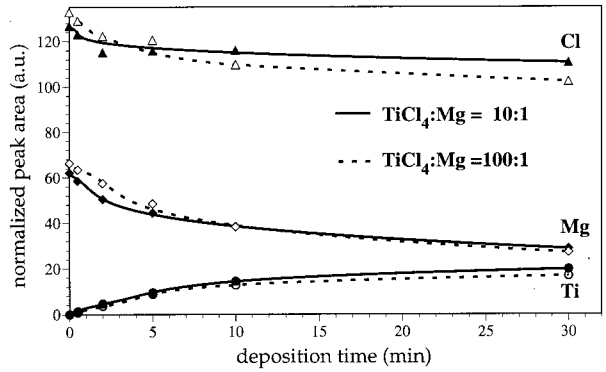

Figure 3. $TiCl_4$ and Mg codeposition on 10 layers of $MgCl_2$ film monitored by XPS as a function of the deposition time. Mg flux: 3×10^{12} atoms/(cm^2 s). Substrate temperature: 300 K. Solid curves: 10:1 $TiCl_4$ to Mg molecular flux ratio at the target surface. Dotted curves: 100:1 $TiCl_4$ to Mg molecular flux ratio at the target surface.

after the exposure of 360 L of $TiCl_4$. This 1 eV shift of the peak maxima can be described as surface charging of the analyzed sample. This charging effect is more intense on the $MgCl_2$ film than after the $TiCl_4$ and Mg codeposition. The Ti 2p region shows the presence of two spin−orbit doublets. Again, the presence of some surface charging induced the shift of the peaks toward lower binding energies as the $TiCl_4$ and Mg exposures increased. The Ti $2p_{3/2}$ peaks with maxima at 459.2 and 456.8 eV after 24 L of $TiCl_4$ shifted to 458.7 and 456.3 eV after 360 L of exposure. These two peaks are respectively assigned to $TiCl_4$ and $TiCl_2$, in agreement with our previous work.[5,6] The same shift in the energy scale is evident in the Mg and Cl peaks.

In Figure 3, the Ti, Mg, and Cl uptakes corresponding to the above-described experiment are reported as a function of the deposition time. In addition, the uptake curves measured during the exposure of the 10 layers of $MgCl_2$ film to a flux of 3×10^{12} Mg atoms/(cm^2 s) and 3×10^{14} $TiCl_4$ molecules/(cm^2 s) are shown. The two sets of curves are not significantly distinct, indicating that in both cases the rate of the film growth was determined by the Mg flux, which was the limiting reagent. A substantial amount of titanium chloride was deposited after 30 min. The surface atomic composition was 12% Ti, 18% Mg, and 70% Cl. In all cases, the deposited films were clean with no detectable traces of oxygen contamination.

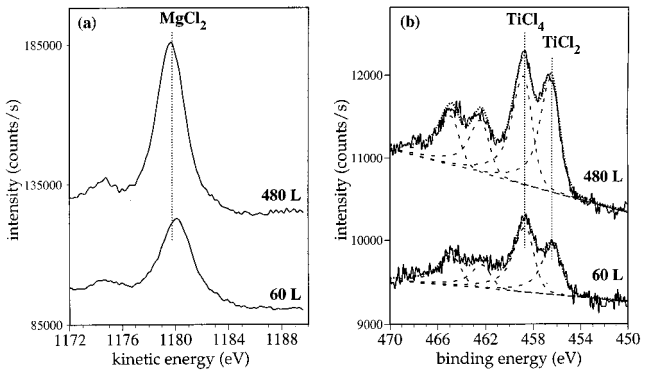

Figure 4. $TiCl_4$ and Mg codeposition on polycrystalline Au. Mg KLL and Ti 2p regions of the XPS spectra at different $TiCl_4$ exposures are shown. $TiCl_4$ pressure: 2×10^{-7} Torr. Mg flux: 3×10^{12} atoms/(cm^2 s). $TiCl_4$ to Mg molecular flux ratio at the target surface: 10:1. Substrate temperature: 300 K. (a) Mg KLL peak. Detector pass energy: 71.5 eV. (b) Ti 2p peak. Detector pass energy: 8.9 eV.

To test the catalytic properties of the $TiCl_4/TiCl_2/MgCl_2$ film prepared by $TiCl_4$ and Mg codeposition, this model system was exposed to a liquid layer of $AlEt_3$ at 360 K for 10 min in the reaction cell. Ethylene was introduced at 760 Torr and polymerized on the catalyst surface at 360 K.

Titanium chloride films of similar quality were grown by $TiCl_4$ and Mg codeposition on polycrystalline Au. We exposed a clean Au foil held at 300 K to a beam of 3×10^{12} Mg atoms/(cm^2 s) in a background pressure of 2×10^{-7} Torr of $TiCl_4$. Figure 4 shows the Mg KLL and Ti 2p XPS peaks after the exposure of 60 and 480 L of $TiCl_4$. The Mg peak with a maximum around 1179.8 eV is probably due to the presence of a chlorine defective $MgCl_2$ or to the formation of a mixed titanium/magnesium chloride ($Ti_\alpha Mg_{1-\alpha}Cl_2$).[5,6] The actual peak position shifted during the deposition experiment toward the value characteristic for $MgCl_2$. The Ti 2p region shows the presence of Ti atoms in two oxidation states. The Ti $2p_{3/2}$ peaks at 458.7 and at 456.4 eV are assigned to $TiCl_4$ and to $TiCl_2$, respectively.

3.3. Mg Deposition on $MgCl_2$ Multilayer Films. Instability of Undercoordinated Mg Surface Atoms. It has been proposed that, during the preparation of the microporous catalyst, $TiCl_4$ chemisorbs on the tetra- and pentacoordinated Mg atoms exposed at the (110) and (100) faces of the $MgCl_2$ crystallites.[1−4] To test this hypothesis, we attempted the preparation of $MgCl_2$ films with a high concentration of undercoordinated Mg atoms at the solid−vacuum interface by exposing a $MgCl_2$ thin film to a beam of Mg atoms.

The atomic beam was produced by a Knudsen cell in which a magnesium rod was maintained at 570 K. The flux of Mg atoms was measured by the rate of deposition of magnesium on a clean gold foil held at 300 K. The change of surface composition was monitored by both XPS and ISS. Figure 5 shows the attenuation of the Au $4f_{7/2}$ peak and the increasing area of the Mg KLL peak during this experiment. The peak areas have been corrected by the respective sensitivity factors. The shape of these curves does not reveal the presence of any evident break, making difficult the determination of the time corresponding to the deposition of one monolayer of magnesium. The ISS uptake analysis showed that the Mg overlayer grew either by the formation of three-dimensional islands or by a Stranski−Krastanov mechanism, as perhaps suggested by the XPS experiment. The ISS spectra recorded after the deposition of different amounts of Mg are reported in Figure 6a and the Au and Mg peak areas are shown in Figure 6b, as a function of

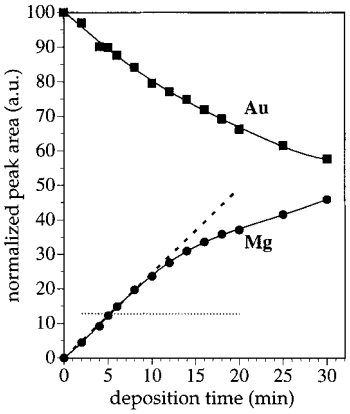

Figure 5. Mg deposition on a polycrystalline Au foil monitored by XPS as a function of the deposition time. Mg source temperature: 570 K. Substrate temperature: 300 K.

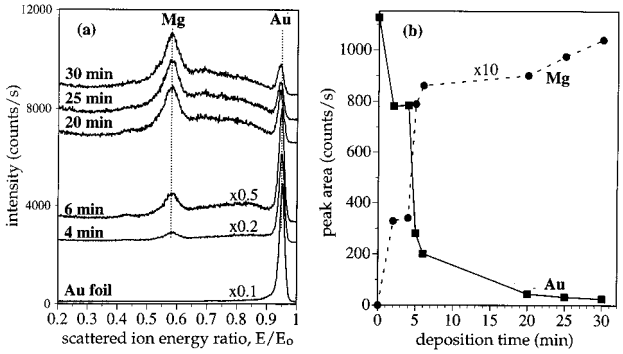

Figure 6. Mg deposition on a polycrystalline Au foil monitored by ISS as a function of the deposition time. Mg source temperature: 570 K. Substrate temperature: 300 K. (a) ISS spectra and (b) Mg and Au peak areas.

the deposition time. After 6 min, the Au peak was about 20% of the peak corresponding to the clean Au surface. At the same time, the Mg peak accounted for 90% of the peak measured after 30 min of deposition.

From the intensity of the Mg XPS peak acquired after the deposition of a thick magnesium film (see section 3.1), we could calculate the intensity of the Mg peak due to one monolayer of Mg atoms at the solid−vacuum interface using the well-known equation[24]

$$i = I[1 - \exp(-t/(\lambda \sin \varphi))]$$

Here, i is the signal intensity due to one monolayer at the interface, I is the signal intensity corresponding to an infinitely thick material, t is the thickness of one monolayer, λ is the inelastic mean free path of the detected electrons, and φ is the takeoff angle. Considering the thickness of one monolayer to be 2.6 Å, half of the c parameter of the hexagonal close-packed unit cell of Mg, and assuming the inelastic mean free path for the 1185.5 eV Mg KLL Auger electrons to be 30 Å,[25] we estimated that the Mg KLL peak due to one monolayer of magnesium deposited on the gold substrate should have a normalized area of approximately 13. This value is represented by the dotted line in Figure 5 and was reached after 5.2 min of deposition.

From the XPS and the ISS analysis we conclude that approximately one monolayer of Mg was deposited in 6 min. Since one monolayer of close-packed Mg atoms has a density of 1.1×10^{15} surface atoms/cm^2, we estimated a Mg deposition rate of approximately 3×10^{12} atoms/(cm^2 s). To calculate

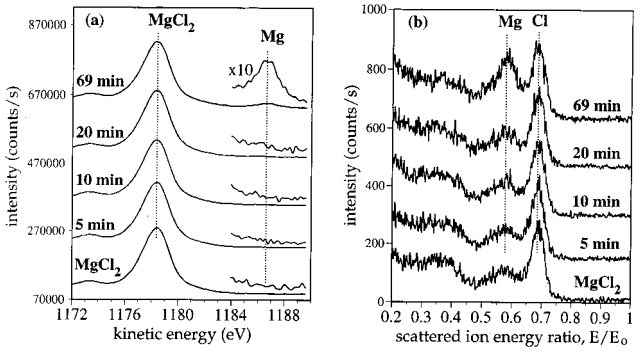

Figure 7. Mg deposition on 10 layers of $MgCl_2$ film monitored by XPS and ISS as a function of the deposition time. Mg flux: 3×10^{12} atoms/(cm^2 s). Substrate temperature: 300 K. (a) Mg KLL XPS peak. The inserts in the high side of the energy scale are multiplied by 10. Detector pass energy: 71.5 eV. (b) ISS spectra.

the flux of Mg atoms at the target surface from the deposition rate, the condensation coefficient of Mg on the Au surface should be determined. However, it is generally accepted that this coefficient for metals on gold at 300 K is unity.[26] Under this assumption, the Mg flux at the target surface coincides with the estimated deposition rate.

The knowledge of the flux was necessary for the precise dosage of the Mg atoms on the magnesium chloride surface, as described below. In the analysis of the results of this last experiment, once again we assume a unity sticking coefficient for Mg on $MgCl_2$ at 300 K. It has been shown that the condensation coefficients for Pt, Pd, and Ir deposited on NaCl between 573 and 673 K are approximately 0.4.[27] The strong dependence of the condensation coefficient on the substrate temperature has been studied in detail in the case of Pd deposition on MgO.[28] Coefficients close to unity have been measured for this system when the substrate was at 430 K. The correct determination of the sticking probability of Mg on the $MgCl_2$ film will be the subject of a future investigation.

The lower curves in Figure 7, parts a and b, respectively show the Mg KLL XPS peak and the ISS spectrum corresponding to 10 layers of $MgCl_2$. The Mg KLL peak has its maximum at 1178.4 eV, as expected for $MgCl_2$. The ISS spectrum shows that the film was Cl terminated, in agreement with our previous results.[9−12] We then exposed this film, held at 300 K, to the Mg atomic beam for 5, 10, 20, and 69 min. Neither the XPS nor the ISS spectra reported in Figure 7 showed any significant modification of the halide surface composition after the deposition of about 4×10^{15} atoms/cm^2. Only after the deposition of 1×10^{16} atoms/cm^2, corresponding to about 10 layers of Mg, a weak peak appeared in the XPS spectrum at 1186.6 eV due to the presence of metallic magnesium. The Mg peak became evident also in the ISS spectrum. The area of the ISS peak was only 11% of the area of the Mg peak measured after the deposition of Mg on Au for 30 min under the same experimental conditions (see Figure 6a). It is worth mentioning that if the actual Mg sticking coefficient on $MgCl_2$ would be only 0.1, the equivalent of about one layer of Mg should be deposited at the halide surface. If this amount of Mg would stay at the solid−vacuum interface, it would be easily detected by both XPS and ISS.

The addition of Mg atoms from the gas phase did not produce a $MgCl_2$ film with a high concentration of surface Mg atoms. Instead, two phases were formed, $MgCl_2$ and metallic Mg. This can be deduced from the analysis of the Mg KLL peak (Figure 7a). The formation of a highly defective, Cl-poor $MgCl_{2-\alpha}$ phase as a consequence of the deposition of Mg on the $MgCl_2$

film can be ruled out because of the lack of a broad peak between 1178.4 and 1186.6 eV. The peak at 1186.6 eV, detected after long Mg exposure, is consistent with the formation of a metallic phase immiscible with $MgCl_2$. The weak intensity of both this peak and the Mg peak in the ISS spectrum (Figure 7b) suggests that the metallic phase must be either embedded in the $MgCl_2$ film or concentrated at the Au surface.

We conclude that Mg-terminated $MgCl_2$ surfaces are unstable under UHV conditions. The high surface energy of this system is the driving force for the diffusion of the Mg adatoms from the surface into the bulk or, more probably, for the diffusion of the subsurface Cl ions to the surface of the halide, to recover the thermodynamically less energetic chlorine termination. According to this second picture, the bulk $MgCl_2$ that loses its Cl ions generates the subsurface Mg phase.

3.4. $TiCl_4$ and $MgCl_2$ Codeposition on Multilayer $MgCl_2$ Films. We have previously reported that the $MgCl_2$ films produced by gas-phase deposition on gold foils grow via a layer-by-layer mechanism.[9,10] The lateral facets of the two-dimensional islands growing at the solid−vacuum interface could, in principle, present a high density of undercoordinated Mg atoms. In fact, we could imagine these Cl−Mg−Cl one-layer facets as segments of $MgCl_2$ faces like, for example, (100) or (110). If these lateral facets were bulk-terminated, we would expect a strong interaction between a Lewis base and the surface Mg atoms. This would cause either the preferential growth of faces other than the basal plane or the inclusion of a substantial amount of the Lewis base in the $MgCl_2$ film during its growth.

To limit the lateral growth of the $MgCl_2$ two-dimensional islands and to favor the expansion of higher Miller index $MgCl_2$ faces, we deposited $MgCl_2$ in the presence of $TiCl_4$ in the vacuum chamber background pressure. A film of 10 layers of $MgCl_2$ previously deposited on a gold foil held at 300 K was simultaneously exposed to $TiCl_4$ and $MgCl_2$. The $MgCl_2$ molecular flux was such that one monolayer of the halide was deposited in 18 min under UHV conditions. From the deposition rate, we estimated a $MgCl_2$ molecular flux of 8×10^{11} molecules/(cm^2 s) at the target surface. The $TiCl_4$ pressure during the codeposition experiment was 5×10^{-7} Torr, corresponding to a flux of 7×10^{13} molecules/(cm^2 s). Under these experimental conditions, approximately 100 molecules of $TiCl_4$ hit the magnesium chloride film per each $MgCl_2$ molecule. Considering that a directed doser was used to bring the gas inlet right in front of the target sample, the actual $TiCl_4$ pressure at the $MgCl_2$ film surface could have been higher than the value measured at the ion gauge. Parts a and b, respectively, of Figure 8 show the Ti 2p region of the XPS spectrum and the Ti 2p, Mg KLL, and Cl 2p uptake curves. The chemical composition of the deposited film remains substantially unchanged during the experiment. Even after the exposure of 450 L of $TiCl_4$, the Ti 2p signal is just above the noise level, indicating a Ti atomic composition of about 0.2%. This corresponds to a sticking probability for $TiCl_4$ on $MgCl_2$ of the order of 10^{-5}, to be compared to a value close to unity for $MgCl_2$ onto itself at room temperature.

4. Discussion

Our experiments show in a direct way that Mg atoms are responsible for the chemisorption of $TiCl_4$ at the $MgCl_2$ surface. Even though the actual sticking coefficient of Mg on $MgCl_2$ at 300 K has not been determined, this should be close to unity. Under this assumption, we have measured by ISS a Mg surface concentration of about 10% after the deposition of the equivalent of 10 layers of Mg on the halide film. Mg atoms are

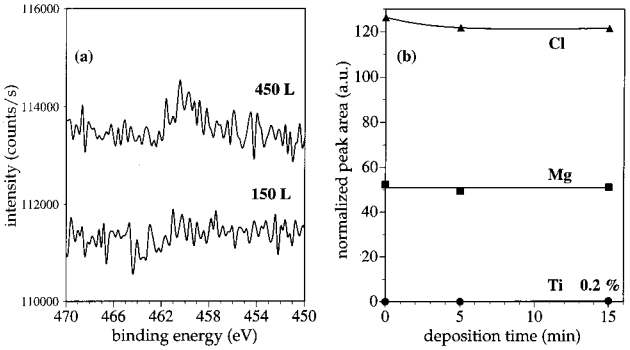

Figure 8. $TiCl_4$ and $MgCl_2$ codeposition on 10 layers of $MgCl_2$ film. $TiCl_4$ pressure: 5×10^{-7} Torr. $MgCl_2$ flux: 8×10^{11} molecules/(cm^2 s). $TiCl_4$ to $MgCl_2$ molecular flux ratio at the target surface: 100:1. Substrate temperature: 300 K. (a) Ti 2p region of the XPS spectra after the exposure of 150 and 450 L of $TiCl_4$. Detector pass energy: 71.5 eV. (b) Ti 2p, Mg KLL, and Cl 2p XPS peak areas as a function of the deposition time.

thermodynamically unstable at the magnesium chloride surface under UHV conditions around room temperature. The high surface energy related to the presence of undercoordinated Mg atoms at the interface is the driving force for the surface reconstruction noticed during the deposition of Mg atoms on $MgCl_2$ multilayer films. The diffusion of Cl ions from the $MgCl_2$ bulk to the surface of the film and their interaction with the Mg atoms deposited from the gas phase are sufficiently fast at 300 K to yield an equilibrated system in the time scale of our experiment. However, the Mg adatoms can be stabilized at the surface of the $MgCl_2$ film when deposited in a background pressure of $TiCl_4$. We can picture the $MgCl_2$ film with a small concentration of undercoordinated surface Mg adatoms as a transient state. $TiCl_4$ molecules chemisorb on this surface by reacting with these Mg atoms. The redox surface reaction between the $TiCl_4$ and the Mg adatoms is faster than the diffusion of the Cl ions from the film bulk. A titanium chloride film composed of $TiCl_4$ and $TiCl_2$ can be grown under these conditions.

The results of our experiments are important to understand, at the molecular level, the role of the $MgCl_2$ as a support for $TiCl_4$. The chlorine ions have a high mobility in the $MgCl_2$ structure and can rapidly diffuse to the surface to correct any defect, such as an undercoordinated Mg surface atom. We would then expect the (100) and (110) faces of $MgCl_2$ to be reconstructed under UHV conditions and expose only Cl atoms at the interface. The long-range order implied by the suggested chemisorption of $TiCl_4$ on the (100) and (110) faces at the lateral cuts of the $MgCl_2$ crystallites would in fact not be present. The sites of $TiCl_4$ chemisorption should then be considered as point defects on the $MgCl_2$ surface. The mobility of the Cl atoms is responsible for the interaction between $MgCl_2$ and different Lewis bases, including $TiCl_4$. In the presence of a Lewis base, the surface Cl atoms can migrate and allow for the formation of stable surface compounds with the reactive Mg atoms. The dynamic nature of the chemistry at the $MgCl_2$ surface is fundamental in the delicate equilibrium between the chemisorption of $TiCl_4$ and the different electron donors used for the synthesis of high-performance catalysts.

Titanium chloride films can be grown under UHV conditions by gas-phase codeposition of $TiCl_4$ and Mg on either $MgCl_2$ or gold around 300 K. Table 3 gives the normalized areas of the Ti 2p, Mg KLL, and Cl 2p peaks measured after different exposures during the $TiCl_4$ and Mg codeposition on the two substrates, together with the surface atomic composition of the deposited overlayer. The deposition of the titanium chloride

TABLE 3: $TiCl_4$ and Mg Codeposition on 10 Layers of $MgCl_2$ and on Polycrystalline Au[a]

substrate	$TiCl_4$ exposure (L)	normalized peak area Ti 2p	Mg KLL	Cl 2p	atomic composition (%) Ti	Mg	Cl
Au foil	60	13.6	8.8	53.3	18	12	70
	480	26.0	20.3	108.6	17	13	70
$MgCl_2$, 10 layers	60	9.5	44.4	115.8	6	26	68
	360	19.7	28.7	110.7	12	18	70

[a] Normalized XPS peak areas and overlayer atomic compositions. $TiCl_4$ flux: 3×10^{14} molecules/(cm^2 s). Mg flux: 3×10^{12} Mg atoms/(cm^2 s). Substrate temperature: 300 K.

film was slightly faster on Au than on $MgCl_2$. Again, this can be explained by the diffusion of the Cl ions from the film bulk to the surface when depositing on $MgCl_2$. In this case, some of the Mg deposited on the film was not available for the redox reaction with $TiCl_4$ to form the titanium chloride film. However, every Mg atom deposited on the Au surface was readily available for the reaction with the $TiCl_4$ to produce the $TiCl_4$/$TiCl_2$/$MgCl_2$ film.

The result of the $TiCl_4$ and $MgCl_2$ codeposition on multilayer $MgCl_2$ films can be interpreted with similar arguments. The high surface energy of $MgCl_2$ films with undercoordinated Mg atoms at the solid−vacuum interface can be lowered by diffusion of Cl atoms to the surface and the full coordination of the outermost Mg atoms. The lateral facets of the two-dimensional islands do not show the bulk termination structure, and $TiCl_4$ cannot chemisorb on them. The result of this experiment is substantially different from that of the $TiCl_4$ and Mg codeposition experiment, where Mg atoms were deposited from the gas phase on the $MgCl_2$ surface. When the $MgCl_2$ molecules impinge on the halide film, they probably can diffuse as $MgCl_2$ entities on the chloride surface, until they find a two-dimensional island to which they adhere. The Mg atom is never exposed to the interface with a geometry favorable for $TiCl_4$ to react with it.

We have described in the present work the synthesis of titanium chloride films by $TiCl_4$ and Mg codeposition on $MgCl_2$ and by the exposure of metallic magnesium to $TiCl_4$. The preparation and characterization of titanium chloride films by electron irradiation induced chemical vapor deposition of $TiCl_4$ on Au and on $MgCl_2$ have been extensively described.[5−8] In all cases, a surface Mg atom appears to be the site for the $TiCl_4$ chemisorption. The successive reaction with an aluminum alkyl produces the active site for the Ziegler−Natta polymerization. The oxidation states of the Ti atoms in the films deposited with these procedures were measured by XPS. The titanium chloride film obtained by gas-phase deposition of $TiCl_4$ on Mg showed a quite complicated stoichiometry, with the titanium atoms in the oxidation states 4+, 3+, 2+, and 0. The relative amount of titanium in the different oxidation states changed with the $TiCl_4$ exposure. The detailed analysis of the film prepared by electron irradiation induced chemical vapor deposition of $TiCl_4$ on $MgCl_2$ thin films revealed the presence of a few layers of $TiCl_2$ with one monolayer of $TiCl_4$ chemisorbed at the surface.[6] The simultaneous deposition of $TiCl_4$ and Mg on $MgCl_2$ produced a film in which the titanium atoms were in the oxidation states 4+ and 2+. Table 4 gives the surface atomic composition of films prepared with the three different methods, and Figure 9 reproduces the Ti 2p region of the corresponding XPS spectra. Because of the different acquisition conditions, the intensities of these spectra cannot be directly compared. The similarity of the spectra corresponding to the films obtained by $TiCl_4$ and Mg codeposition and by electron irradiation induced

TABLE 4: XPS Surface Atomic Compositions of the Titanium Chloride Films Deposited by (a) $TiCl_4$ Exposure to Mg, (b) $TiCl_4$ Electron-Induced Deposition on $MgCl_2$, and (c) $TiCl_4$ and Mg Codeposition on $MgCl_2$[a]

deposition method	atomic composition (%) Ti	Mg	Cl	O
(a) $TiCl_4$ exposure to Mg film	16	20	62	2
(b) $TiCl_4$ electron-induced deposition on $MgCl_2$	27	0	73	0
(c) $TiCl_4$ and Mg codeposition on $MgCl_2$	12	18	70	0

[a] Deposition conditions are as for Figure 9.

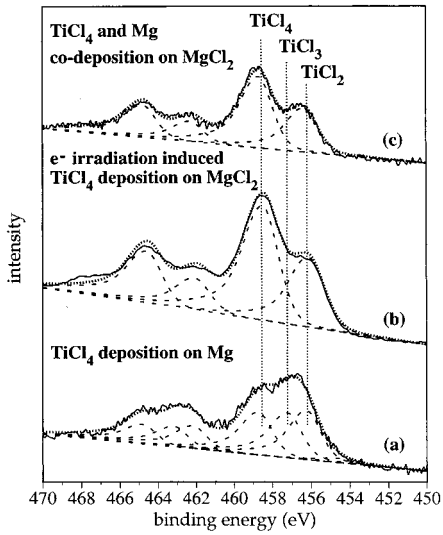

Figure 9. Ti 2p region of the XPS spectra of titanium chloride films deposited at 300 K by three different methods. The curve fitting of the experimental spectra is shown. (a) Exposure of a Mg film to 1000 L of $TiCl_4$. $TiCl_4$ pressure: 1×10^{-6} Torr. Detector pass energy: 8.9 eV. (b) Electron irradiation induced $TiCl_4$ deposition on 10 layers of $MgCl_2$ film. $TiCl_4$ exposure: 240 L. $TiCl_4$ pressure: 2×10^{-7} Torr. Electron flux: 3×10^{14} electrons/(cm^2 s). Electron energy: 1 keV. Detector pass energy: 71.5 eV. (c) $TiCl_4$ and Mg codeposition on 10 layers of $MgCl_2$ film. $TiCl_4$ exposure: 360 L. $TiCl_4$ pressure: 2×10^{-7} Torr. Mg flux: 3×10^{12} atoms/(cm^2 s). $TiCl_4$ to Mg molecular flux ratio at the target surface: 10:1. Detector pass energy: 8.9 eV.

$TiCl_4$ deposition is quite evident. In both cases, the titanium atoms are present in oxidation states 4+ and 2+. However, the amounts of Mg present in the films prepared with these two methods are substantially different. While no Mg was detected by XPS in the film obtained by electron irradiation induced deposition, about 18% of Mg was present in the film prepared by codeposition of $TiCl_4$ and Mg. The redox surface reaction between $TiCl_4$ and Mg produced a mixture of $TiCl_2$ and $MgCl_2$. Because of the similarity of the crystallographic structures of $MgCl_2$ and $TiCl_2$,[29−31] a mixed titanium/magnesium chloride with titanium in the 2+ oxidation state ($Ti_\alpha Mg_{1-\alpha}Cl_2$) might be formed during the codeposition experiment. According to this interpretation, films b and c of Figure 9 and Table 4 would only differ in their subsurface composition, being pure $TiCl_2$ in film b and a mixed titanium/magnesium chloride in film c. In both cases, $TiCl_4$ is strongly chemisorbed at the film surface.

It appears that the $TiCl_4$/$TiCl_2$/$MgCl_2$ film is quite stable at room temperature, being formed by means of two substantially different synthetic methods. In particular, the $TiCl_4$ and Mg codeposition makes use of Mg atoms at conventional thermal energy, as opposed to the irradiation of the $MgCl_2$ film with electrons of 1 keV of energy. This new chemical method for the synthesis of titanium chloride films could allow us to prepare

titanium chloride films of uniform composition and surface structure. Our goal is to obtain in this way a single-site heterogeneous Ziegler−Natta catalyst.

5. Conclusions

We studied the chemisorption of $TiCl_4$ molecules on a clean Mg surface. Titanium chloride films could be deposited in this way with the Ti atoms in the 4+, 3+, 2+, and 0 oxidation states. The composition of this film is quite complex and depends on the $TiCl_4$ exposure. Upon reaction with $AlEt_3$, this film became an active catalyst for the Ziegler−Natta polymerization of ethylene and propylene. With this experiment, we proved the XPS analysis suitable for the quantitative determination of $TiCl_4$, $TiCl_3$, and $TiCl_2$ species simultaneously present at the sample surface.

$MgCl_2$ surfaces with high concentrations of undercoordinated Mg atoms are unstable under UHV conditions. The Mg adatoms deposited from the gas phase on a multilayer $MgCl_2$ film were readily coordinated by the Cl ions diffusing from the halide bulk to the surface to lower the surface energy of the system. The $MgCl_2$ film was predominantly Cl-terminated after the deposition of an equivalent of 10 layers of metallic Mg. This is an important direct evidence of the dynamic behavior of the $MgCl_2$ surface at 300 K and of the instability of $MgCl_2$ faces other than the basal plane under UHV conditions.

The Mg adatoms deposited on the $MgCl_2$ film were stabilized at the film surface in the presence of $TiCl_4$ in the gas phase. In this case, the Mg adatoms reacted with the $TiCl_4$ molecules from the gas phase before the Cl ions diffusing from the film bulk could coordinate to the Mg atoms at the interface. Our experiments show conclusively that surface magnesium atoms are responsible for the chemisorption of $TiCl_4$ and the formation of the precursor of the polymerization reaction active sites. The redox surface reaction between the $TiCl_4$ molecules and the Mg atoms produced a mixture of $TiCl_2$ and $MgCl_2$ with a monolayer of $TiCl_4$ molecules chemisorbed at the surface. A similar $TiCl_4$/$TiCl_2$/$MgCl_2$ film was produced by $TiCl_4$ and Mg codeposition on a gold foil. The XPS analysis indicated that the titanium chloride films obtained by $TiCl_4$ and Mg codeposition were very similar to the ones obtained by electron irradiation-induced $TiCl_4$ deposition. We suggest that the $TiCl_4$/$TiCl_2$ system is highly stable at room temperature. Both model systems became active Ziegler−Natta catalysts after the reaction with $AlEt_3$.

Finally, we tried to enhance the growth of high Miller index faces of $MgCl_2$ by depositing magnesium chloride in the presence of a large excess of $TiCl_4$. Titanium chloride could not be deposited under these conditions. This is indicative of the absence of any Mg at the growing $MgCl_2$ film surface. This result can be interpreted, once again, in view of the high surface energy of $MgCl_2$ faces with undercoordinated Mg atoms at the solid−vacuum interface.

Acknowledgment. This work was supported by the Director, Office of Energy Research, Office of Basic Energy Sciences, Materials Sciences Division, of the U.S. Department of Energy under Contract No. DE-AC03-76SF00098. The authors also acknowledge support from Montell USA, Inc.

References and Notes

(1) Dusseault, J. J. A.; Hsu, C. C. *J. Macromol. Sci., Rev. Macromol. Chem. Phys.* **1993**, *C33*, 103.
(2) Corradini, P.; Guerra, G. *Prog. Polym. Sci.* **1991**, *16*, 239.
(3) Barbè, P. C.; Cecchin, G.; Noristi, L. *Adv. Polym. Sci.* **1986**, *81*, 1.
(4) Giannini, U.; Giunchi, G.; Albizzati, E.; Barbè, P. C. *Recent Advances in Mechanistic and Synthetic Aspects of Polymerization*; Fontanille, M., Guyot, A., Eds.; NATO ASI Series, Vol. 215; D. Reidel Publishing Co.: Dordrecht, The Netherlands, 1987; p 473.
(5) Magni, E.; Somorjai, G. A. *Surf. Sci.* **1996**, *345*, 1.
(6) Magni, E.; Somorjai, G. A. *J. Phys. Chem.* **1996**, *100*, 14786.
(7) Magni, E.; Somorjai, G. A. *Surf. Sci.* **1997**, *377*, 824.
(8) Magni, E.; Somorjai, G. A. *Catal. Lett.* **1995**, *35*, 205.
(9) Magni, E.; Somorjai, G. A. *Appl. Surf. Sci.* **1995**, *89*, 187.
(10) Magni, E.; Somorjai, G. A. *Surf. Sci.* **1995**, *341*, L1078.
(11) Fairbrother, D. H.; Roberts, J. G.; Rizzi, S.; Somorjai, G. A. *Langmuir* **1997**, *13*, 2090.
(12) Roberts, J. G.; Gierer, M.; Fairbrother, D. H.; Van Hove, M.; Somorjai, G. A. *Surf. Sci.* **1998**, *399*, 123.
(13) Moulder, J. F.; Stickle, W. F.; Sobol, P. E.; Bomben, K. D. *Handbook of X-ray Photoelectron Spectroscopy*; Physical Electronics, Inc.: Eden Prairie, MN, 1995.
(14) The tail used for the description of the asymmetric XPS peaks has the mathematical form

$$\mathrm{TS}\{1 - \exp[-\mathrm{LN}(2)(2(X_i - \mathrm{PP})/\mathrm{fwhm})^2]\} \times \exp\{(-6.9/\mathrm{TL})[2(X_i - \mathrm{PP})/\mathrm{fwhm}]\}$$

where X_i is the binding energy value of the ith data point, PP is the binding energy of the peak center, and the remaining symbols are explained in the text. The curve fitting with synthetic peaks of this mathematical form is easily accessible using the software provided with our PHI 5400 ESCA system.
(15) Ley, L.; McFeely, F. R.; Kowalczyk, S. P.; Jenkin, J. G.; Shirley, D. A. *Phys. Rev. B* **1975**, *11*, 600.
(16) Steiner, P.; Reiter, F. J.; Hoechst, H.; Huefner, S.; Fuggle, J. C. *Phys. Lett.* **1978**, *66 A*, 229.
(17) Fuggle, J. C. *Surf. Sci.* **1977**, *69*, 581.
(18) Hoogewijs, R.; Fiermans, L.; Vennik, J. *J. Electron Spectrosc. Relat. Phenom.* **1977**, *11*, 171.
(19) Fuggle, J. C.; Watson, L. M.; Fabian, D. J.; Affrossman, S. *J. Phys. F. Met. Phys.* **1975**, *5*, 375.
(20) Garbassi, F.; Pozzi, L. *J. Electron Spectrosc. Relat. Phenom.* **1979**, *16*, 199.
(21) Seyama, H.; Soma, M. *Chem. Lett.* **1981**, *7*, 1009.
(22) Mousty-Desbuquoit, C.; Riga, J.; Verbist, J. J. *Inorg. Chem.* **1987**, *26*, 1212.
(23) Mousty-Desbuquoit, C.; Riga, J.; Verbist, J. J. *J. Chem. Phys.* **1983**, *79*, 26.
(24) Briggs, D.; Seah, M. P. *Practical Surface Analysis. Volume 1—Auger and X-ray Photoelectron Spectroscopy*, 2nd ed.; J. Wiley & Sons: Chichester, U.K., 1990.
(25) Tanuma, S.; Powell, C. J.; Penn, D. R. *Surf. Interface Anal.* **1991**, *17*, 911.
(26) Ohring, M. *The Materials Science of Thin Films*; Academic Press: London, 1992.
(27) Rupprechter, G.; Hayek, K.; Rendón, L.; José-Yacamán, M. *Thin Solid Films* **1995**, *260*, 148.
(28) Henry, C. R.; Chapon, C.; Duriez, C.; Giorgio, S. *Surf. Sci.* **1991**, *253*, 177.
(29) Bassi, I. W.; Polato, F.; Calcaterra, M.; Bart, J. C. J. *Z. Kristallogr.* **1982**, *159*, 297.
(30) Baenziger, N. C.; Rundle, R. E. *Acta Crystallogr.* **1948**, *1*, 274.
(31) Gal'perin, E. L.; Sandler, R. A. *Kristallografiia* **1962**, *7*, 217.